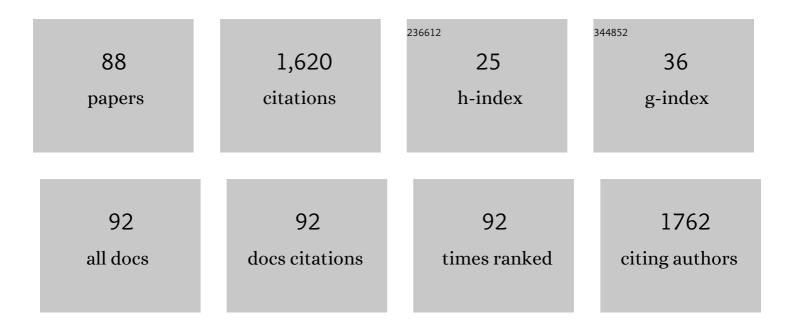
Lucia Romano

List of Publications by Year in descending order

Source: https://exaly.com/author-pdf/6078891/publications.pdf Version: 2024-02-01



#	Article	IF	CITATIONS
1	High aspect ratio tilted gratings through local electric field modulation in plasma etching. Applied Surface Science, 2022, 588, 152938.	3.1	9
2	Fabrication of a fractal pattern device for focus characterizations of X-ray imaging systems by Si deep reactive ion etching and bottom-up Au electroplating. Applied Optics, 2022, 61, 3850.	0.9	5
3	Optimization of displacement Talbot lithography for fabrication of uniform high aspect ratio gratings. Japanese Journal of Applied Physics, 2021, 60, SCCA01.	0.8	12
4	Fabrication of X-ray Gratings for Interferometric Imaging by Conformal Seedless Gold Electroplating. Micromachines, 2021, 12, 517.	1.4	14
5	Laboratory X-ray interferometry imaging with a fan-shaped source grating. Optics Letters, 2021, 46, 3693.	1.7	9
6	High sensitivity X-ray phase contrast imaging by laboratory grating-based interferometry at high Talbot order geometry. Optics Express, 2021, 29, 2049.	1.7	35
7	Editorial for the Special Issue on Micro- and Nano-Fabrication by Metal Assisted Chemical Etching. Micromachines, 2020, 11, 988.	1.4	0
8	Towards the Fabrication of High-Aspect-Ratio Silicon Gratings by Deep Reactive Ion Etching. Micromachines, 2020, 11, 864.	1.4	36
9	Highâ€Aspectâ€Ratio Grating Microfabrication by Platinumâ€Assisted Chemical Etching and Gold Electroplating. Advanced Engineering Materials, 2020, 22, 2000258.	1.6	32
10	Microfabrication of X-ray Optics by Metal Assisted Chemical Etching: A Review. Micromachines, 2020, 11, 589.	1.4	36
11	Metal assisted chemical etching of silicon in the gas phase: a nanofabrication platform for X-ray optics. Nanoscale Horizons, 2020, 5, 869-879.	4.1	50
12	Pushing the Limits of Bottom-Up Gold Filling for X-ray Grating Interferometry. Journal of the Electrochemical Society, 2020, 167, 132504.	1.3	20
13	Towards sub-micrometer high aspect ratio X-ray gratings by atomic layer deposition of iridium. Microelectronic Engineering, 2018, 192, 19-24.	1.1	39
14	Development of Laboratory Grating-based X-ray Phase Contrast Microtomography for Improved Pathology. Microscopy and Microanalysis, 2018, 24, 192-193.	0.2	6
15	High-intensity x-ray microbeam for macromolecular crystallography using silicon kinoform diffractive lenses. Applied Optics, 2018, 57, 9032.	0.9	5
16	High aspect ratio metal microcasting by hot embossing for X-ray optics fabrication. Microelectronic Engineering, 2017, 176, 6-10.	1.1	27
17	Effect of isopropanol on gold assisted chemical etching of silicon microstructures. Microelectronic Engineering, 2017, 177, 59-65.	1.1	35
18	High-aspect ratio silicon structures by displacement Talbot lithography and Bosch etching. Proceedings of SPIE, 2017, , .	0.8	18

Lucia Romano

#	Article	IF	CITATIONS
19	Photoactive layered nanocomposites obtained by direct transferring of anodic TiO 2 nanotubes to commodity thermoplastics. Applied Surface Science, 2017, 399, 451-462.	3.1	8
20	Hot embossing of Au- and Pb-based alloys for x-ray grating fabrication. Journal of Vacuum Science and Technology B:Nanotechnology and Microelectronics, 2017, 35, .	0.6	14
21	Measuring fusion excitation functions with RIBs using the stacked target technique: Problems and possible solutions. EPJ Web of Conferences, 2016, 117, 06013.	0.1	0
22	A generalized quantitative interpretation of dark-field contrast for highly concentrated microsphere suspensions. Scientific Reports, 2016, 6, 35259.	1.6	27
23	Single-crystal TiO ₂ nanowires by seed assisted thermal oxidation of Ti foil: synthesis and photocatalytic properties. RSC Advances, 2016, 6, 55490-55498.	1.7	5
24	Immobilization of nanomaterials in PMMA composites for photocatalytic removal of dyes, phenols and bacteria from water. Journal of Photochemistry and Photobiology A: Chemistry, 2016, 321, 1-11.	2.0	71
25	Self-assembly nanostructured gold for high aspect ratio silicon microstructures by metal assisted chemical etching. RSC Advances, 2016, 6, 16025-16029.	1.7	37
26	PMMA/TiO2 nanotubes composites for photocatalytic removal of organic compounds and bacteria from water. Materials Science in Semiconductor Processing, 2016, 42, 58-61.	1.9	27
27	TiO2 nanowires on Ti thin film for water purification. Materials Science in Semiconductor Processing, 2016, 42, 24-27.	1.9	15
28	Sub-barrier radioactive ion beam investigations using a new methodology and analysis for the stacked target technique. Physical Review C, 2015, 92, .	1.1	17
29	Measuring fusion excitation functions with RIBs: A thorough analysis of the stacked target technique and the related problems. AIP Conference Proceedings, 2015, , .	0.3	0
30	Optical Properties of Nanoporous Germanium Thin Films. ACS Applied Materials & Interfaces, 2015, 7, 16992-16998.	4.0	24
31	UV-black rutile TiO2: An antireflective photocatalytic nanostructure. Journal of Applied Physics, 2015, 117, 074903.	1.1	22
32	C ion-implanted TiO2 thin film for photocatalytic applications. Journal of Applied Physics, 2015, 117, .	1.1	35
33	Photocatalytical and antibacterial activity of TiO2 nanoparticles obtained by laser ablation in water. Applied Catalysis B: Environmental, 2015, 165, 487-494.	10.8	109
34	Correlation Between Structural and Sensing Properties of Carbon Nanotube-Based Devices. Lecture Notes in Electrical Engineering, 2015, , 207-210.	0.3	1
35	Fe ion-implanted TiO2 thin film for efficient visible-light photocatalysis. Journal of Applied Physics, 2014, 116, .	1.1	35
36	Millisecond infrared laser irradiation of SiO <inf>x</inf> N <inf>y</inf> : the role of nitrogen in the photoluminescence emission. , 2014, , .		0

LUCIA ROMANO

#	Article	IF	CITATIONS
37	TiO2-coated nanostructures for dye photo-degradation in water. Nanoscale Research Letters, 2014, 9, 458.	3.1	55
38	An enhanced photocatalytic response of nanometric TiO ₂ wrapping of Au nanoparticles for eco-friendly water applications. Nanoscale, 2014, 6, 11189-11195.	2.8	58
39	Structural and optical properties of solid-state synthesized Au dendritic structures. Applied Surface Science, 2014, 296, 177-184.	3.1	4
40	Optoelectronic properties of nanoporous Ge layers investigated by surface photovoltage spectroscopy. Microporous and Mesoporous Materials, 2014, 196, 175-178.	2.2	11
41	Influence of microstructure on voids nucleation in nanoporous Ge. Materials Letters, 2013, 96, 74-77.	1.3	10
42	Nanoporous Ge coated by Au nanoparticles for electrochemical application. Electrochemistry Communications, 2013, 30, 83-86.	2.3	6
43	Heavy residue excitation functions for the collisions6,7Li+64Zn near the Coulomb barrier. Physical Review C, 2013, 87, .	1.1	45
44	Molybdenum sputtering film characterization for high gradient accelerating structures. Chinese Physics C, 2013, 37, 097005.	1.5	7
45	Structural and morphological characterization of Mo coatings for high gradient accelerating structures. Journal of Physics: Conference Series, 2013, 430, 012091.	0.3	2
46	High-temperature annealing of thin Au films on Si: Growth of SiO2 nanowires or Au dendritic nanostructures?. Applied Physics Letters, 2012, 100, .	1.5	26
47	Nanoporous Ge electrode as a template for nano-sized (< 5 nm) Au aggregates. Nanotechnology, 2012, 23, 395604.	1.3	13
48	Nanoporosity induced by ion implantation in deposited amorphous Ge thin films. Journal of Applied Physics, 2012, 111, .	1.1	35
49	Development of X-band accelerating structures for high gradients. Chinese Physics C, 2012, 36, 639-647.	1.5	7
50	Activation and thermal stability of ultra-shallow B+-implants in Ge. Journal of Applied Physics, 2012, 112, 123525.	1.1	3
51	Nanoporosity Induced by Ion Implantation in Germanium Thin Films Grown by Molecular Beam Epitaxy. Applied Physics Express, 2012, 5, 035201.	1.1	22
52	Characterisation of solid-phase-epitaxy of amorphous germanium thin-films. , 2012, , .		0
53	Towards a laser fluence dependent nanostructuring of thin Au films on Si by nanosecond laser irradiation. Applied Surface Science, 2012, 258, 9128-9137.	3.1	37
54	p-type conduction in ion-implanted amorphized Ge. Materials Science in Semiconductor Processing, 2012, 15, 703-706.	1.9	8

LUCIA ROMANO

#	Article	IF	CITATIONS
55	Novel approach to the fabrication of Au/silica core–shell nanostructures based on nanosecond laser irradiation of thin Au films on Si. Nanotechnology, 2012, 23, 045601.	1.3	52
56	A Combined Ion Implantation/Nanosecond Laser Irradiation Approach towards Si Nanostructures Doping. Journal of Nanotechnology, 2012, 2012, 1-6.	1.5	7
57	Nanoscale amorphization, bending and recrystallization in silicon nanowires. Applied Physics A: Materials Science and Processing, 2011, 102, 13-19.	1.1	33
58	Formation and evolution of small B clusters in Si: Ion channeling study. Physical Review B, 2010, 81, .	1.1	3
59	High-level incorporation of antimony in germanium by laser annealing. Journal of Applied Physics, 2010, 108, .	1.1	38
60	Nanostructuring in Ge by self-ion implantation. Journal of Applied Physics, 2010, 107, .	1.1	66
61	Amorphization of Si using cluster ions. Journal of Vacuum Science & Technology B, 2009, 27, 597.	1.3	8
62	Nanoscale manipulation of Ge nanowires by ion irradiation. Journal of Applied Physics, 2009, 106, .	1.1	38
63	Electrical Activation and Carrier Compensation in Si and Mg Implanted GaN by Scanning Capacitance Microscopy. Solid State Phenomena, 2008, 131-133, 491-496.	0.3	8
64	Role of the strain in the epitaxial regrowth rate of heavily doped amorphous Si films. Applied Physics Letters, 2008, 93, .	1.5	9
65	<i>In situ</i> thermal evolution of B–B pairs in crystalline Si: a spectroscopic high resolution x-ray diffraction study. Journal of Physics Condensed Matter, 2008, 20, 175215.	0.7	2
66	Substitutional B in Si: Accurate lattice parameter determination. Journal of Applied Physics, 2007, 101, 093523.	1.1	13
67	Physical insight into the phenomenon of B clustering in Si at room temperature. Nuclear Instruments & Methods in Physics Research B, 2007, 257, 146-151.	0.6	4
68	Amorphous–crystalline interface evolution during Solid Phase Epitaxy Regrowth of SiGe films amorphized by ion implantation. Nuclear Instruments & Methods in Physics Research B, 2007, 257, 270-274.	0.6	1
69	Quantitative determination of depth carrier profiles in ion-implanted Gallium Nitride. Nuclear Instruments & Methods in Physics Research B, 2007, 257, 336-339.	0.6	16
70	Role of Si self-interstitials on the electrical de-activation of B doped Si. Nuclear Instruments & Methods in Physics Research B, 2006, 242, 656-658.	0.6	1
71	Fluorine incorporation during Si solid phase epitaxy. Nuclear Instruments & Methods in Physics Research B, 2006, 242, 614-616.	0.6	2
72	Group III impurities – Si interstitials interaction caused by ion irradiation. Nuclear Instruments & Methods in Physics Research B, 2006, 242, 646-649.	0.6	2

LUCIA ROMANO

#	Article	IF	CITATIONS
73	Room-temperature B off-lattice displacement and electrical deactivation induced by H and He implantation. Nuclear Instruments & Methods in Physics Research B, 2006, 249, 181-184.	0.6	5
74	Mechanism of de-activation and clustering of B in Si at extremely high concentration. Nuclear Instruments & Methods in Physics Research B, 2006, 253, 50-54.	0.6	9
75	Lattice strain of B–B pairs formed by He irradiation in crystalline Si1â^'xBx/Si. Nuclear Instruments & Methods in Physics Research B, 2006, 253, 55-58.	0.6	2
76	Carrier mobility and strain effect in heavily doped p-type Si. Materials Science and Engineering B: Solid-State Materials for Advanced Technology, 2006, 135, 220-223.	1.7	6
77	Effect of Strain on the Carrier Mobility in Heavily Dopedp-Type Si. Physical Review Letters, 2006, 97, 136605.	2.9	13
78	Boron lattice location in room temperature ion implanted Si crystal. Materials Science and Engineering B: Solid-State Materials for Advanced Technology, 2005, 124-125, 249-252.	1.7	5
79	B implanted at room temperature in crystalline Si: B defect formation and dissolution. Materials Science and Engineering B: Solid-State Materials for Advanced Technology, 2005, 124-125, 253-256.	1.7	0
80	Impurities–Si interstitials interaction in Si doped with B or Ga during ion irradiation. Journal of Physics Condensed Matter, 2005, 17, S2279-S2284.	0.7	2
81	Cross section of the interaction between substitutional B and Si self-interstitials generated by ion beams. Journal of Physics Condensed Matter, 2005, 17, S2273-S2277.	0.7	2
82	Influence of point defects injection on the stability of a supersaturatedGa‣isolid solution. Physical Review B, 2005, 71, .	1.1	6
83	Lattice location and thermal evolution of small B complexes in crystalline Si. Applied Physics Letters, 2005, 87, 201905.	1.5	9
84	Room-temperature boron displacement in crystalline silicon induced by proton irradiation. Applied Physics Letters, 2005, 86, 081906.	1.5	17
85	Fluorine segregation and incorporation during solid-phase epitaxy of Si. Applied Physics Letters, 2005, 86, 121905.	1.5	30
86	Electrical activation and lattice location of B and Ga impurities implanted in Si. Nuclear Instruments & Methods in Physics Research B, 2004, 219-220, 727-731.	0.6	4
87	Structural characterization and oxygen concentration profiling of a Co/Si multilayer structure. Nuclear Instruments & Methods in Physics Research B, 2004, 219-220, 732-736.	0.6	0
88	Carrier concentration and mobility in B doped Si1â^'xGex. Materials Science and Engineering B: Solid-State Materials for Advanced Technology, 2003, 102, 49-52.	1.7	20